Cell Reports, Volume *25*

Supplemental Information

Drp1 Controls Effective T Cell Immune-Surveillance by Regulating T Cell Migration, Proliferation, and cMyc-Dependent Metabolic Reprogramming

Luca Simula, Ilenia Pacella, Alessandra Colamatteo, Claudio Procaccini, Valeria Cancila, Matteo Bordi, Claudia Tregnago, Mauro Corrado, Martina Pigazzi, Vincenzo Barnaba, Claudio Tripodo, Giuseppe Matarese, Silvia Piconese, and Silvia Campello

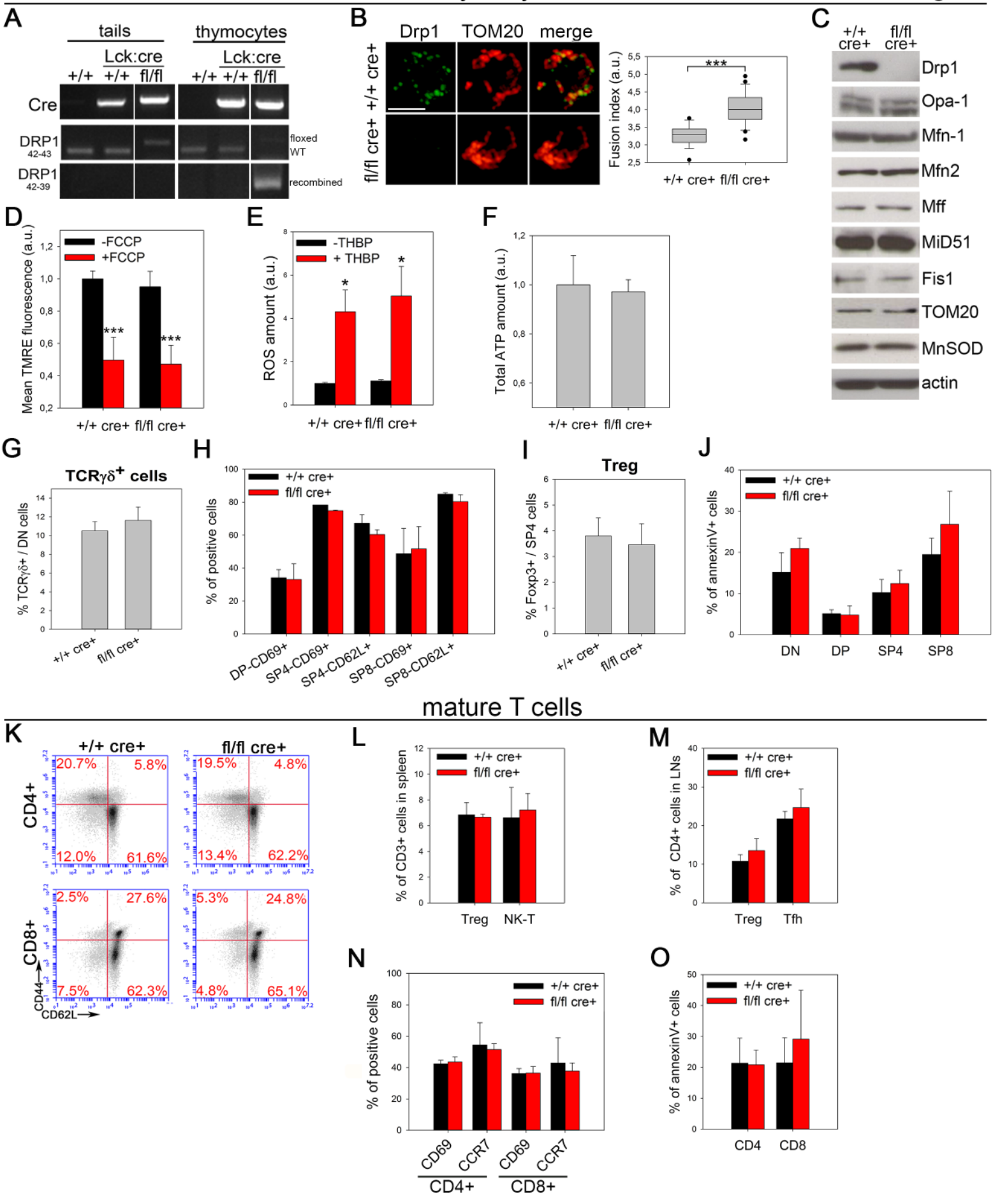
A
tails
thymocytes
Lck:cre
+/+ +/+ fl/fl
Cre
DRP1 42-43
DRP1 42-39
floxed
WT
recombined
B
Drp1
TOM20
merge
+/+ cre+
fl/fl cre+
Fusion index (a.u.)
***
+/+ cre+ fl/fl cre+
C
+/+ cre+
fl/fl cre+
Drp1
Opa-1
Mfn-1
Mfn2
Mff
MiD51
Fis1
TOM20
MnSOD
actin
D
-FCCP
+FCCP
Mean TMRE fluorescence (a.u.)
+/+ cre+ fl/fl cre+
E
-THBP
+ THBP
ROS amount (a.u.)
+/+ cre+ fl/fl cre+
F
Total ATP amount (a.u.)
+/+ cre+ fl/fl cre+
G
TCRγδ+ cells
% TCRγδ+ / DN cells
+/+ cre+
fl/fl cre+
H
+/+ cre+
fl/fl cre+
% of positive cells
DP-CD69+
SP4-CD69+
SP4-CD62L+
SP8-CD69+
SP8-CD62L+
I
Treg
% Foxp3+ / SP4 cells
+/+ cre+
fl/fl cre+
J
+/+ cre+
fl/fl cre+
% of annexinV+ cells
DN
DP
SP4
SP8
mature T cells
K
+/+ cre+
fl/fl cre+
CD4+
CD8+
20.7%
5.8%
12.0%
61.6%
19.5%
4.8%
13.4%
62.2%
2.5%
27.6%
7.5%
62.3%
5.3%
24.8%
4.8%
65.1%
CD44
CD62L
L
+/+ cre+
fl/fl cre+
% of CD3+ cells in spleen
Treg
NK-T
M
+/+ cre+
fl/fl cre+
% of CD4+ cells in LNs
Treg
Tfh
N
+/+ cre+
fl/fl cre+
% of positive cells
CD69
CCR7
CD69
CCR7
CD4+
CD8+
O
+/+ cre+
fl/fl cre+
% of annexinV+ cells
CD4
CD8

Supplemental Figure 1. Tissue specific deletion of Drp1 protein in T cell lineage impairs thymocyte mitochondrial fragmentation but does not interfere with the cell type relative distribution in primary or secondary lymphoid organs. Related to Figure 1.

(A) PCR genotyping of +/+ cre+ control and fl/fl cre+ Drp1 KO mice (n=3). Note that the thymocytes and the tails were run on separate gels. (**B**) z-stack reconstruction of confocal images of mitochondria (TOM20, in red) and Drp1 (in green) expression in +/+ cre+ control and fl/fl cre+ Drp1 KO thymocytes. Quantification of mitochondrial morphology by fusion index is reported in the graph (at least 90 cells from three mice per group) (n=3). (**C**) Western Blot analysis of mitochondrial shaping proteins and mitochondrial markers levels in +/+ cre+ control and fl/fl cre+ Drp1 KO thymocytes (Drp1, Mfn1 n=7; Opa-1, n=4; TOM20, MnSOD, n=6; Mfn2, MiD51, Mff, Fis1, n=3). (**D**) Measurement of mitochondrial potential ($\Delta\psi$) by mean TMRE fluorescence in +/+ cre+ control and fl/fl cre+ Drp1 KO thymocytes. FCCP has been used as positive control for $\Delta\psi$ depolarization (n=5). (**E**) Flow cytometric measurement of ROS amounts (DCFDA mean fluorescence index) in +/+ cre+ control and fl/fl cre+ Drp1 KO thymocytes. TBHP has been used as positive control for ROS production (n=5). (**F**) Total ATP amounts in +/+ cre+ control and fl/fl cre+ Drp1 KO thymocytes (n=5). (**G**, **H**, **I** and **J**) Cytofluorimetric measurement of the percentage of DN TCR$\gamma\delta^+$ (G, n=4), CD69$^+$ and CD62L$^+$ cells (H, n=3), SP4 Treg cells (I, n=3) and annexin V+ subsets (J, n=4) in +/+ cre+ control and fl/fl cre+ Drp1 KO thymocytes. (**K**) Cytofluorimetric measurement of the percentage of CD4+ and CD8+ subsets according to CD62L and CD44 expression in +/+ cre+ control and fl/fl cre+ Drp1 KO T cells (n=6). (**L**) Cytofluorimetric measurement of the percentage of Treg and Natural Killer T (NK-T) cells in +/+ cre+ control and fl/fl cre+ Drp1 KO CD3+ T cells isolated from spleen (B, n=3). (**M**) Cytofluorimetric measurement of the percentage of Treg (n=3) and CD4+ CXCR5+PD1+ T follicular helper cells (Tfh) (n=3) in +/+ cre+ control and fl/fl cre+ Drp1 KO CD4+ T cells in lymph node pool. (**N**) Cytofluorimetric measurement of the percentage of CCR7$^+$ and CD69$^+$ cells in +/+ cre+ control and fl/fl cre+ Drp1 KO CD4+ and CD8+ T cells isolated from lymph node pool. (**O**) Percentage of annexinV+ cells in +/+ cre+ control and fl/fl cre+ Drp1 KO CD4+ and CD8+ T cells isolated from spleen (n=6).
Data are represented as mean ± SEM. Scale bar, 10μm. Significance is indicated as follows: *=p<0.05, ***= p<0.001.

Fig. S2

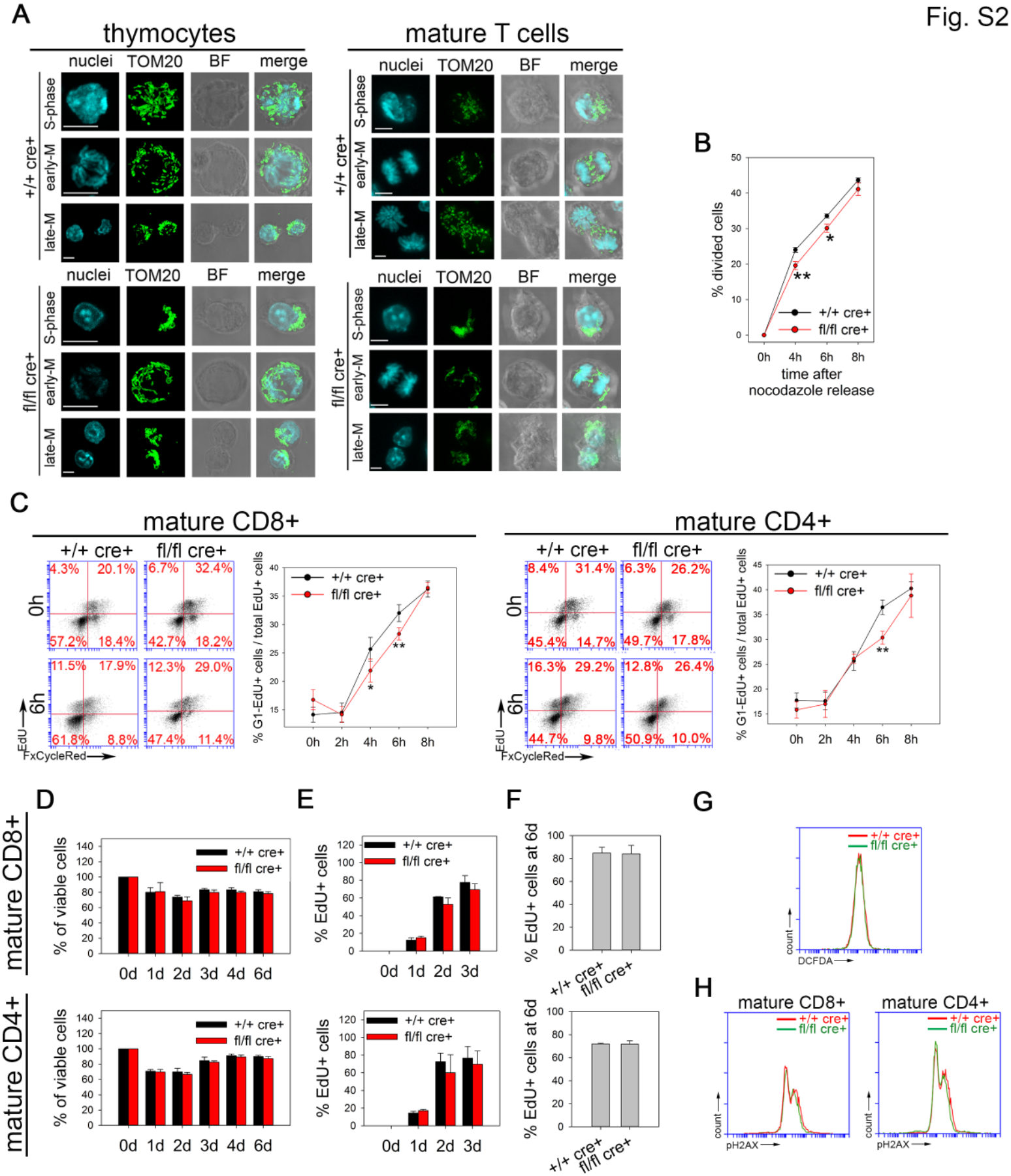
A
thymocytes
mature T cells
nuclei
TOM20
BF
merge
+/+ cre+
fl/fl cre+
S-phase
early-M
late-M
B
% divided cells
+/+ cre+
fl/fl cre+
time after nocodazole release
C
mature CD8+
mature CD4+
0h
6h
EdU
FxCycleRed
% G1-EdU+ cells / total EdU+ cells
D
E
F
G
H
mature CD8+
mature CD4+
% of viable cells
% EdU+ cells
% EdU+ cells at 6d
count
DCFDA
pH2AX

Supplemental Figure 2. Further analysis of proliferation in thymocytes and mature T cells. Related to Figure 2.

(**A**) z-stack reconstruction of confocal images of mitochondrial (TOM20, in green) morphology in +/+ cre+ control and fl/fl cre+ Drp1 KO thymocytes stimulated with PHA and IL2 for 3 days (n=3) or in control and Drp1 KO CD4+ T cells after 6 days of *in vitro* activation (n=3) during different phases of cell cycle. (**B**) Release from o.n. nocodazole block for CFSE stained thymocytes pre-activated *in vitro* for 3 days. Percentage of divided cells (halving of CFSE mean fluorescence) for each indicated time point is shown in the graph (n=4 ctrl, n=5 KO). (**C**) Analysis of EdU incorporation and DNA content (FxCycle Red staining) in *in vitro*-activated CD8+ (n=7) and CD4+ (n=5) T cells, after 30min EdU pulse. Quantification of EdU^+ cells (%) with G1 DNA content among the total EdU^+ cells is shown in the graphs. (**D**) Percentage of $annexinV^-$ CD8+ and CD4+ +/+ cre+ control and fl/fl cre+ Drp1 KO T cells during 6 days of *in vitro* activation (n=5). (**E**) Cytofluorimetric measurement of the percentage of proliferating cells after 2h EdU pulse given to +/+ cre+ control and fl/fl cre+ Drp1 KO CD8+ and CD4+ T cells at 0-1-2-3 days after *in vitro* activation (n=2). (**F**) Cytofluorimetric measurement of the percentage of proliferating cells after 24h EdU pulse given to +/+ cre+ control and fl/fl cre+ Drp1 KO CD8+ and CD4+ T cells 6 days after *in vitro* activation (n=3). (**G**) ROS amounts measured as DCFDA fluorescence in +/+ cre+ and fl/fl cre+ Drp1 KO CD3+ T cells 6 days after *in vitro* stimulation (n=3). (**H**) Percentage of +/+ cre+ and fl/fl cre+ Drp1 KO CD8+ and CD4+ T cells positive for phospho-H2AX flow-cytometric staining 6 days after *in vitro* stimulation (n=3).
Data are represented as mean ± SEM. Scale bar, 5μm. Significance is indicated as follows: *=$p<0.05$, **=$p<0.01$.

Fig. S3

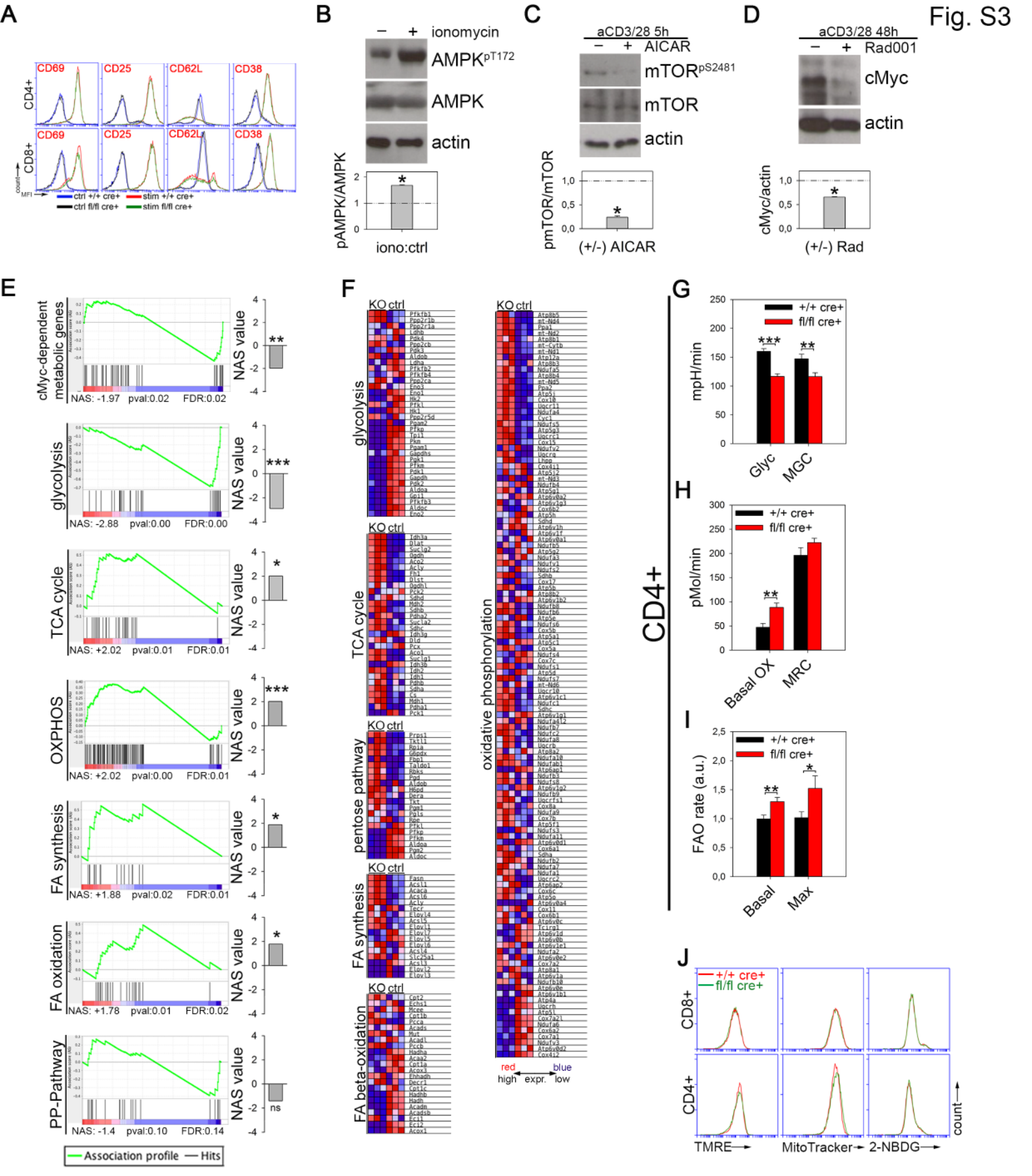
A
CD69
CD25
CD62L
CD38
CD4+
CD8+
ctrl +/+ cre+
stim +/+ cre+
ctrl fl/fl cre+
stim fl/fl cre+
B
ionomycin
AMPKpT172
AMPK
actin
pAMPK/AMPK
iono:ctrl
C
aCD3/28 5h
AICAR
mTORpS2481
mTOR
actin
pmTOR/mTOR
(+/-) AICAR
D
aCD3/28 48h
Rad001
cMyc
actin
cMyc/actin
(+/-) Rad
E
cMyc-dependent metabolic genes
glycolysis
TCA cycle
OXPHOS
FA synthesis
FA oxidation
PP-Pathway
NAS value
NAS: -1.97 pval:0.02 FDR:0.02
NAS: -2.88 pval:0.00 FDR:0.00
NAS: +2.02 pval:0.01 FDR:0.01
NAS: +2.02 pval:0.00 FDR:0.01
NAS: +1.88 pval:0.02 FDR:0.01
NAS: +1.78 pval:0.01 FDR:0.02
NAS: -1.4 pval:0.10 FDR:0.14
ns
Association profile
Hits
F
KO ctrl
glycolysis
TCA cycle
pentose pathway
FA synthesis
FA beta-oxidation
oxidative phosphorylation
red
blue
high expr. low
G
+/+ cre+
fl/fl cre+
mpH/min
Glyc
MGC
H
pMol/min
Basal OX
MRC
I
FAO rate (a.u.)
Basal
Max
CD4+
J
CD8+
CD4+
TMRE
MitoTracker
2-NBDG
count
K
+/+ cre+
fl/fl cre+
Drp1
ATPb
actin
CD8
CD4
L
ATP amounts (a.u.)
M
MFI relative to control
IL7Ra
CD44
IFNg
TNFa
IL2
Tb/Em
IL4
th0
th1
th2
N
% of IFNg released per cell

Supplemental Figure 3. Further analysis of metabolic reprogramming in mature T cells. Related to Figure 3.

(**A**) Expression profile of CD69, CD62L (control: day zero; stimulated: day one), CD38 and CD25 (control: day zero; stimulated: day two) for *in vitro* activated T cells (n=3). (**B-C-D**) Western blot analysis of the indicated (phospho)-protein levels from wild-type T cells stimulated *in vitro* with ionomycin for 1h (B, n=3), aCD3 plate-coated plus CD28/IL2, with or without AICAR for 5h (C, n=3) or Rad-001 for 48h (D, n=3). (**E-F**) +/+ cre+ control and fl/fl cre+ Drp1 KO T cells have been activated for 3 days *in vitro* and then processed for RNA seq. GSAA enrichment plot of the expression level of the indicated group of genes (E) and corresponding raw heatmap data (F). See also Supplemental Table. Related to Fig. 3F-G (NAS: normalized association score; pval=normalized p-value; FDR: false discovery rate) (n=3). (**G-H-I**) Seahorse analysis of ECAR (G) and OCR (H-I) values in +/+ cre+ control and fl/fl cre+ Drp1 KO CD4+ T cells 6 days after *in vitro* activation (2-DG: 2-deoxyglucose; Rot/an; Rotenone/antimycin). For evaluation of fatty acid oxidation, OCR rate has been measured with BSA-palmitate, with or without etomoxir (I). The following parameters have been quantified: glycolysis(Glyc), maximal glycolytic capacity (MGC); basal OXPHOS (Basal OX), maximum respiratory capacity (MRC), basal (Basal) and maximal (Max) fatty acid oxidation. (n=3). (**J**) Measurement of the Mean fluorescence index (MFI) for Mitotracker, TMRE and 2-NBDG in +/+ cre+ control and fl/fl cre+ Drp1 KO T cells 6 days after *in vitro* activation (Mitotracker, TMRE n=6; 2-NBDG, n=4). (**K**) Western blot analysis of the mitochondrial marker ATPb expression in +/+ cre+ control and fl/fl cre+ Drp1 KO T cells 6 days after *in vitro* activation (n=2). (**L**) Total ATP amounts in +/+ cre+ control and fl/fl cre+ Drp1 KO CD3+ T cells 6 days after *in vitro* activation (n=3). (**M**) Cytofluorimetric measurements of the Mean fluorescence index (MFI) for IL7Ra (n=11), CD44 (n=8), KLRG1 (n=9), IFNγ (n=10), TNFα (n=6), IL2 (n=4), IL4 (n=7) and for the Tbet:Eomes MFIs ratio (n=8) in +/+ cre+ control and fl/fl cre+ Drp1 KO CD4+ splenic T cells upon 6 days of *in vitro* activation under the indicated polarizing conditions (see Materials and Methods for details). (**N**) Percentage of IFNγ released by +/+ cre+ control and fl/fl cre+ Drp1 KO CD8+ T cells after *in vitro* re-stimulation with a-CD3/CD28 antibodies 6d after initial activation (n=3). The following formula has been applied: [(IFNγ mean fluorescence index, MFI, with monensin) - (IFNγ MFI without monensin)] / (IFNγ MFI with monensin).
Data are represented as mean ± SEM. Significance is indicated as follows: * = p< 0.05, **=p<0.01, ***= p<0.001.

Fig. S4

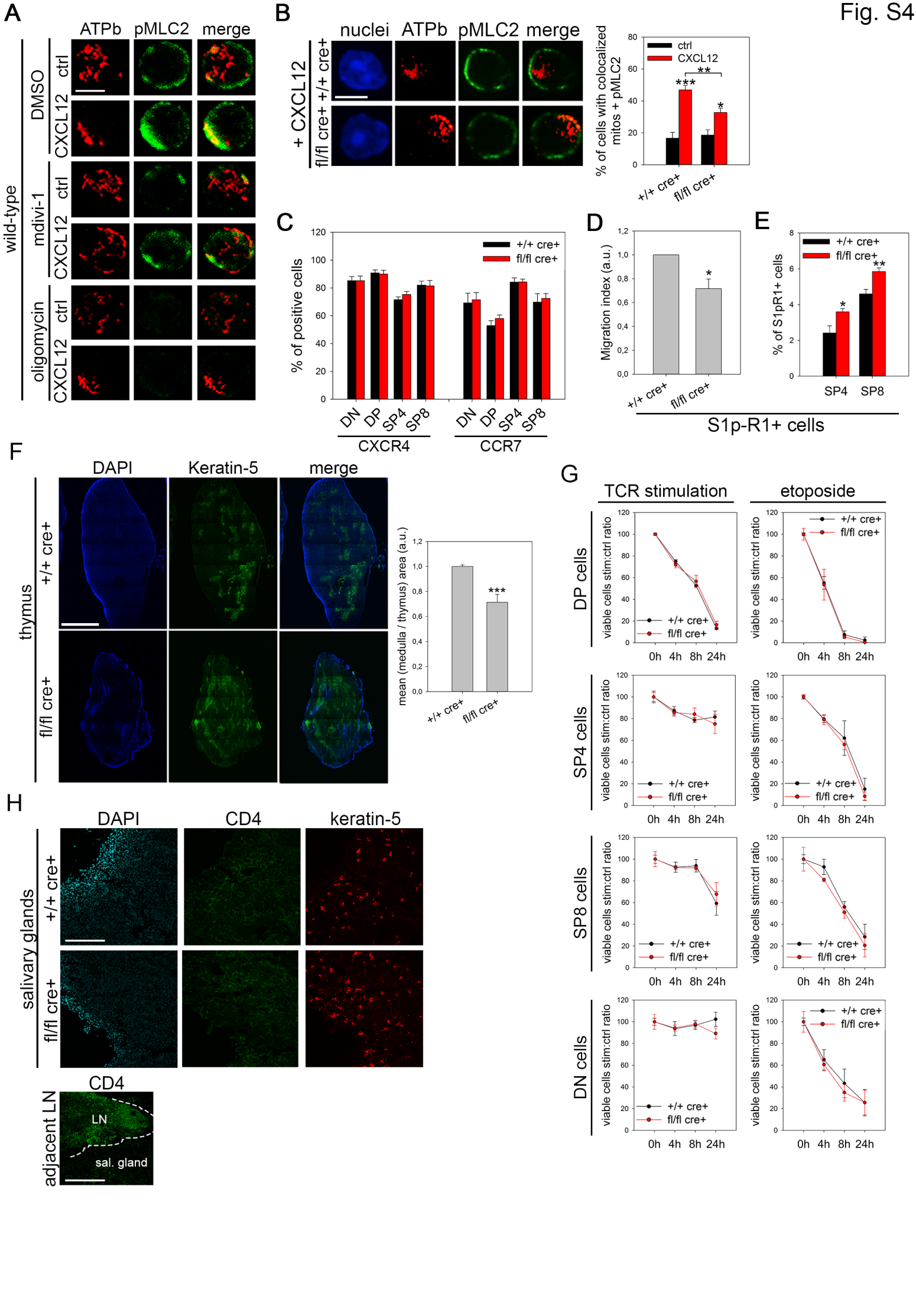
A
ATPb
pMLC2
merge
wild-type
DMSO
ctrl
CXCL12
mdivi-1
ctrl
CXCL12
oligomycin
ctrl
CXCL12
B
nuclei
ATPb
pMLC2
merge
+ CXCL12
fl/fl cre+ +/+ cre+
% of cells with colocalized mitos + pMLC2
ctrl
CXCL12
***
**
*
+/+ cre+
fl/fl cre+
C
% of positive cells
+/+ cre+
fl/fl cre+
DN
DP
SP4
SP8
CXCR4
CCR7
D
Migration index (a.u.)
*
+/+ cre+
fl/fl cre+
S1p-R1+ cells
E
% of S1pR1+ cells
+/+ cre+
fl/fl cre+
*
**
SP4
SP8
F
DAPI
Keratin-5
merge
thymus
+/+ cre+
fl/fl cre+
mean (medulla / thymus) area (a.u.)
***
+/+ cre+
fl/fl cre+
G
TCR stimulation
etoposide
DP cells
SP4 cells
SP8 cells
DN cells
viable cells stim:ctrl ratio
+/+ cre+
fl/fl cre+
0h
4h
8h
24h
H
DAPI
CD4
keratin-5
salivary glands
+/+ cre+
fl/fl cre+
CD4
adjacent LN
LN
sal. gland

Supplemental Figure 4. Further analysis of migration in thymocytes. Drp1 conditional KO mice show reduction in medullary islets' mean area, increased TUNEL+ cell density not dependent on a differential apoptotic response and absence of autoreactive T infiltrates into salivary glands. Related to Figure 4.

(**A**) z-stack reconstruction of confocal images of mitochondria (ATPb, in red) and phospho-MLC2 (in green) in wild type thymocytes treated with DMSO, mdivi-1 or oligomycin and then stimulated with 50nM CXCL12 (n=6). (**B**) z-stack reconstruction of confocal images of mitochondria (ATPb, in red) and pMLC2 (in green) localization in +/+ cre+ control and fl/fl cre+ Drp1 KO thymocytes stimulated with 50nM CXCL12. The percentage of cells with colocalizing mitochondria and pMLC2 is reported in the graph (n=8). (**C**) Cytofluorimetric analysis of the percentage of cells positive for CCR7 or CXCR4 in +/+ cre+ control and fl/fl cre+ Drp1 KO thymocytes subsets (n=3). (**D** and **E**) Cytofluorimetric analysis of the percentage of S1p-R1^{+} cells (d, n=4) and transwell migration assay in presence of 100nM S1p (e, n=4) for +/+ cre+ control and fl/fl cre+ Drp1 KO single positive thymocytes. (**F**) Quantification of the ratio between mean medullary islets (Keratin-5^{+}) section area and thymus area in +/+ cre+ control and fl/fl cre+ Drp1 KO thymic sections (n=5). z-stack reconstruction of confocal images for Keratin-5 expression. (**G**) Quantification of the stimulated:control viability ratio in +/+ cre+ control and fl/fl cre+ Drp1 KO thymocyte subsets stimulated *in vitro* with anti-TCRβ/CD28/CD2 antibodies (n=4) or with 50μMM etoposide (n=4) for the indicated time. (**H**) Salivary gland sections from +/+ cre+ control and fl/fl cre+ Drp1 KO mice immunostained with anti-CD4 (to visualize infiltrating CD4 T cells) and anti-Keratin5 (to stain acinar tubules) antibodies. Adjacent lymph node was used as positive control for anti-CD4 immunostaining (n=3).
Data are represented as mean ± SEM. Scale bar, 5μm in **A** and **B**, 2mm in **F** and 200μm in **H**. Significance is indicated as follows: * = $p< 0.05$, ** = $p<0.01$, *** = $p<0.001$.

Fig. S5

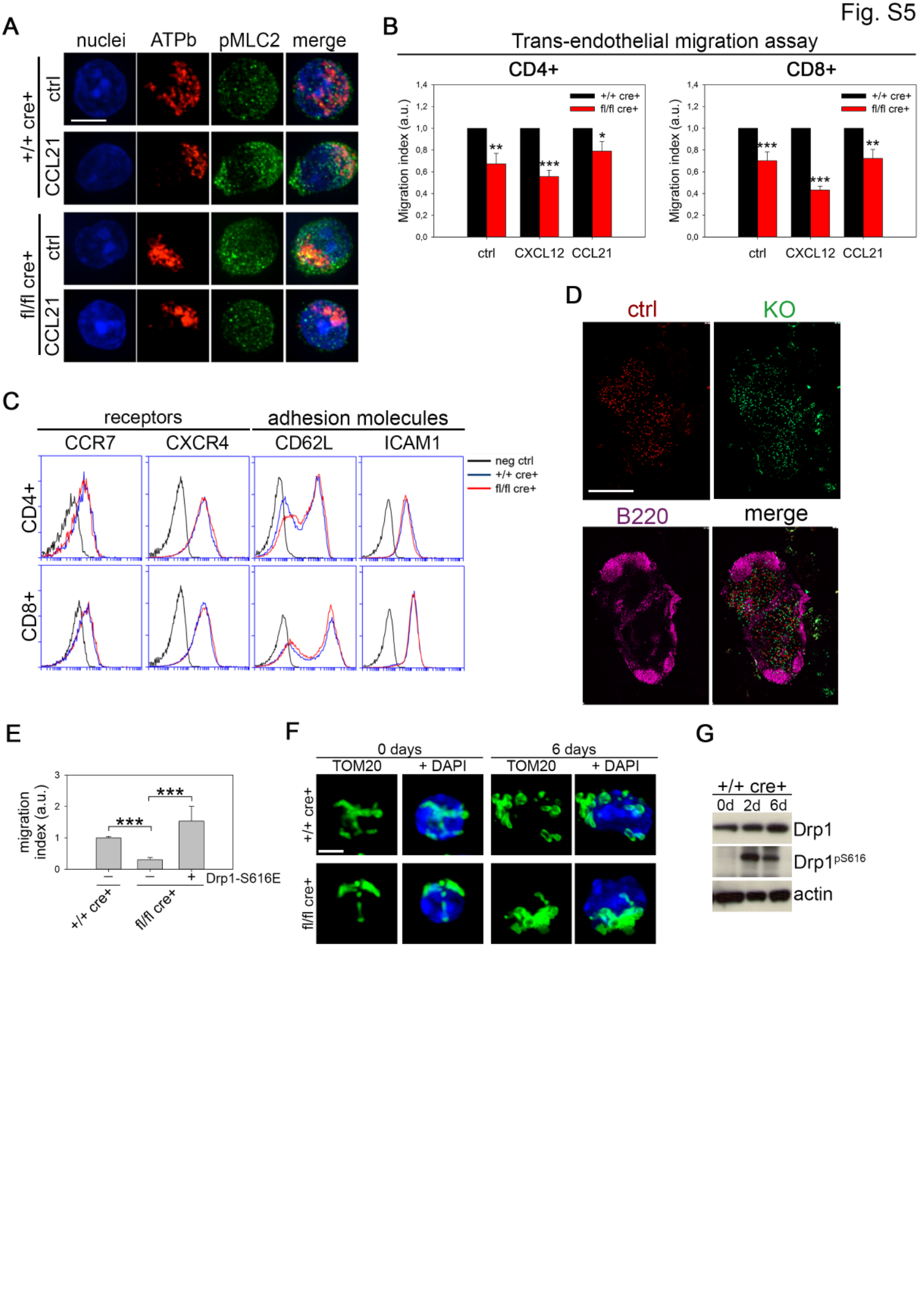
A
nuclei
ATPb
pMLC2
merge
+/+ cre+
fl/fl cre+
ctrl
CCL21
B
Trans-endothelial migration assay
CD4+
CD8+
Migration index (a.u.)
+/+ cre+
fl/fl cre+
ctrl
CXCL12
CCL21
C
receptors
adhesion molecules
CCR7
CXCR4
CD62L
ICAM1
CD4+
CD8+
neg ctrl
+/+ cre+
fl/fl cre+
D
ctrl
KO
B220
merge
E
migration index (a.u.)
Drp1-S616E
+/+ cre+
fl/fl cre+
F
0 days
6 days
TOM20
+ DAPI
+/+ cre+
fl/fl cre+
G
+/+ cre+
0d
2d
6d
Drp1
Drp1pS616
actin

Supplemental Figure 5. Further analysis of migration and Drp1-dependent fragmentation in mature T cells. Related to Figure 5.

(**A**) z-stack reconstruction of confocal images of mitochondria (ATPb, in red) localization and pMLC2 (in green) expression in 6 days *in vitro* activated +/+ cre+ control and fl/fl cre+ Drp1 KO T cells stimulated with 50nM CCL21 (n=3). (**B**) Transwell migration assay of *in vitro* activated +/+ cre+ control or fl/fl cre+ Drp1 KO T cells, with or without 50nM of CXCL12 or CCL21 in presence of an endothelial monolayer. The number of migrating cells normalized to the control population is reported for both CD4+ and CD8+ T cells in each condition (ctrl, CCL21 n=11; CXCL12, n=5). (**C**) Cytofluorimetric analysis of the expression levels of CXCR4 and CCR7 receptors, CD62L and ICAM1 adhesion molecules in +/+ cre+ control and fl/fl cre+ Drp1 KO 6 days *in vitro* activated CD4+ and CD8+ T cells (n=7). (**D**) Intravenous injection of 1:1 *in vitro* activated +/+ cre+ control (eFluor 670-labelled) and fl/fl cre+ Drp1 KO (CFSE-labelled) T cells into WT recipient. After 24h, lymph nodes have been isolated from recipient mice and fixed for immunostaining. Localization of control (eFluor 670) and Drp1 KO (CFSE) T cells inside T (B220-) and B (B220+) cell zones of recipient inguinal lymph node (n=9). (**E**) +/+ cre+ control and fl/fl cre+ Drp1 KO T cells have been activated 6 days *in vitro* and then electroporated with either empty vector pEYFP-C1 or with pEYFP-C1-Drp1-S616E plasmids (only KO cells). After 24 hours, migration of the cells has been analysed in transwell assays in presence of 50nM CCL21 chemokine for 2 hours (gating on YFP+ cells) (n=6). (**F**) z-stack reconstructions of mitochondrial morphology (TOM20, in green) in +/+ cre+ control and fl/fl cre+ Drp1 KO T cells immediately after isolation (0 days) and 6 days after activation (6 days) (n=3). (**G**) Western blot analysis of (phospho)-Drp1 levels in wild type T cells activated *in vitro* 2 days and then expanded for additional 4 days with only IL2 (n=3).
Data are represented as mean ± SEM. Scale bar 10μm in **A,** 5 μm in **F** and 500μm in **D**. Significance is indicated as follows: * = $p< 0.05$, ** = $p<0.01$.

Fig. S6

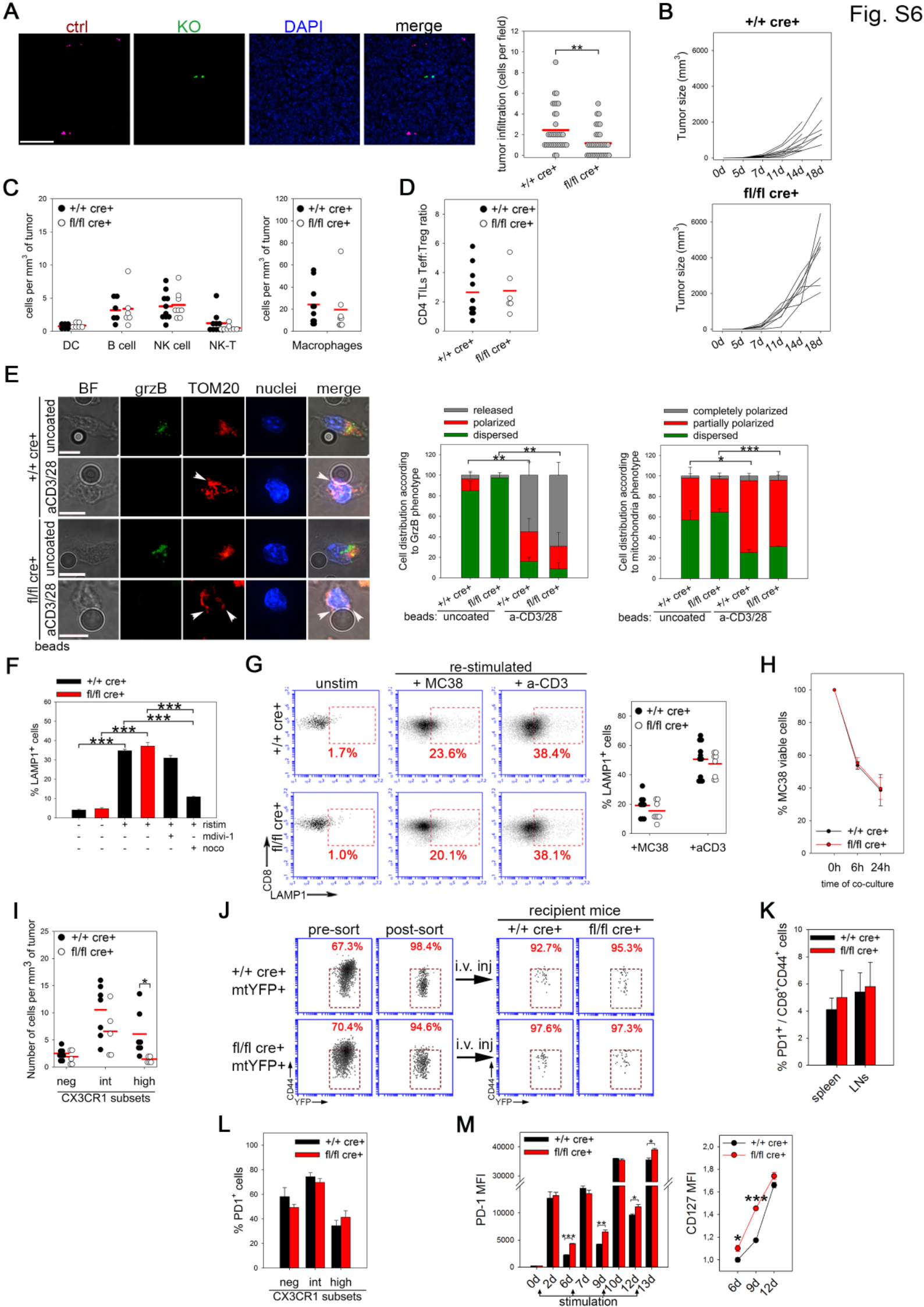
A
ctrl
KO
DAPI
merge
tumor infiltration (cells per field)
+/+ cre+
fl/fl cre+
B
+/+ cre+
Tumor size (mm3)
0d 5d 7d 11d 14d 18d
fl/fl cre+
C
cells per mm3 of tumor
DC
B cell
NK cell
NK-T
Macrophages
D
CD4 TILs Teff:Treg ratio
E
BF
grzB
TOM20
nuclei
merge
uncoated
aCD3/28
beads
released
polarized
dispersed
Cell distribution according to GrzB phenotype
completely polarized
partially polarized
Cell distribution according to mitochondria phenotype
beads: uncoated
a-CD3/28
F
% LAMP1+ cells
ristim
mdivi-1
noco
G
unstim
re-stimulated
+ MC38
+ a-CD3
1.7%
23.6%
38.4%
1.0%
20.1%
38.1%
CD8
LAMP1
+MC38
+aCD3
H
% MC38 viable cells
0h 6h 24h
time of co-culture
I
Number of cells per mm3 of tumor
neg
int
high
CX3CR1 subsets
J
pre-sort
post-sort
recipient mice
67.3%
98.4%
92.7%
95.3%
70.4%
94.6%
97.6%
97.3%
i.v. inj
mtYFP+
CD44
YFP
K
% PD1+ / CD8+CD44+ cells
spleen
LNs
L
% PD1+ cells
M
PD-1 MFI
CD127 MFI
0d 2d 6d 7d 9d 10d 12d 13d
stimulation
6d 9d 12d

Supplemental Figure 6. Further analysis of T cells infiltration into MCA38-induced subcutaneous tumors and functional analysis of cytotoxicity in isolated Drp1 KO T cells. Related to Figure 6.

(**A**) *In vitro* activated control (eFluor670-labelled) and Drp1 KO (CFSE-labelled) T cells were injected i.v. into WT recipient mice in which MC38-subcutaneous tumors were induced 13days before. After 24 hours tumor masses were collected and the exogenous control and KO TILs' density on tumor slices was quantified by immunofluorescence (H) (Data shown are representative of 1 of 2 independent experiments; 30 fields/mouse analysed at 20x; here, the fluorescence signal shown, corresponding to "control" and "KO" cells, is enhanced through a mask filter used by Volocity software to clearly identify positive cells). (**B**) Growth curves of MCA38-induced subcutaneous tumor in single +/+ cre+ control and fl/fl cre+ Drp1 conditional KO mice (n=11 ctrl, 8 KO). (**C**) Number of dendritic cells (DC), B cells (B), natural killer (NK), natural killer-T (NK-T) and macrophages per mm^3 of MC38-derived tumor 18 days after subcutaneous injection (DC, B cells, n=6 ctrl, 6 KO; NK, NK-T, n=10 ctrl, 8 KO). (**D**) Effector:Regulatory T cell ratio among CD4+ TILs into MC38-derived tumors 18 days after subcutaneous injection (n=10 ctrl, 6 KO). (**E**) Mitochondria (TOM20, red) and granzymeB (green) distribution in +/+ cre+ control and fl/fl cre+ Drp1 KO CD8+ T cells 4h after re-stimulation with uncoated or a-CD3/CD28-coated beads. Arrows indicate point of contact between mitochondrial network coated-beads. Graphs on the right report the distribution of cells according to granzymeB (dispersed, polarized close to the bead, released/absent) or mitochondria morphology (widely dispersed, partially polarized toward the bead (as shown in figure for coated-beads) or completely polarized toward the bead) (n=4). (**F**) Percentage of LAMP1 positive cells in +/+ cre+ control and fl/fl cre+ Drp1 KO CD8+ T cells either left unstimulated or re-stimulated for 4 hours with a-CD3/CD28 antibodies, 6d after initial activation (n=4). +/+ cre+ control T cells have been also pre-treated for 1h with Drp1 inhibitor mdivi-1 (50μM) or with nocodazole (30μM) (added also during the re-stimulation) (n=4). (**G**) Splenocytes from MC38-bearing +/+ cre+ control and fl/fl cre+ Drp1 conditional KO CD8+ mice have been isolated and expanded *in vitro* for 10d with IL2, IL15 and UV-irradiated MC38 cells (last two days without MC38 cells). Then CD8+ T cells have been magnetically sorted and either left unstimulated or restimulated with a-CD3/CD28 antibodies (+a-CD3) or MC38 cells (+MC38) for 6 hours. Dot plots and the graph on the right report the percentage of LAMP1 positive cells in the different conditions (n=9 ctrl, 8 KO). (**H**) Viability of MC38 cells 6 or 24 hours after co-culture with +/+ cre+ control or fl/fl cre+ Drp1 KO CD8+ T cells (obtained as described in **G**) (n=9 ctrl, 8 KO). (**I**) Absolute number of +/+ cre+ control and fl/fl cre+ Drp1 KO CD8+ TILs inside tumor mass distinguished according to CX3CR1 expression (n=8 ctrl, 5 KO). (**J**) +/+ cre+ mtYFP+/+ control and fl/fl cre+ mtYFP+/+ Drp1 KO CD3+ T cells have been isolated from spleen (pre-sort) and naïve $CD44^-$ T cells purified with magnetic sorting (post-sort). Then cells have been injected i.v. into +/+ cre+ control and fl/fl cre+ Drp1 conditional KO mice and harvested after 10 days from spleen. The percentage of exogenous mtYFP+ cells expressing the memory marker CD44 is reported for each condition (n = at least 3 recipient mice for each condition). (**K**) Percentage of PD-1 positive cells among CD8+ CD44+ T cells freshly isolated from spleen and lymph nodes of +/+ cre+ control and fl/fl cre+ Drp1 conditional KO mice (n=3 ctrl, 2 KO). (**L**) Percentage of PD-1 positive cells among CX3CR1 subsets (negative, intermediate, high) in CD8+ TILs isolated from MC38-derived tumors 18 days after subcutaneous injection in +/+ cre+ control and fl/fl cre+ Drp1 conditional KO mice (n=6). (**M**) PD1 and CD127 mean fluorescence index (MFI) in +/+ cre+ control and fl/fl cre+ Drp1 KO T cells isolated from spleen (day 0) and then stimulated *in vitro* at the indicated days (arrows) for 24 hours (only the first stimulation lasted for 48 hours) and left in IL2 for the rest of time (n=3).
Data are represented as mean ± SEM in **E**, **F**, **H**, **K**, **L** and **M** and as dot density plot in **A**, **C**, **D**, **G** and **I**. Scale bar, 80μm in **A** and 10μm in **E**. Significance is indicated as follows: * = $p< 0.05$, ** = $p<0.01$, *** = $p<0.001$.

TABLE S1

Glycolysis			
Gene	**baseMean**	**Log2(FC)**	**padj**
Aldoa	103491,44	-0,723	8,29E-26
Aldob	0,475	0,027	NA
Aldoc	5183,226	-0,942	8,75E-45
Eno1	38419,091	-0,313	9,75E-07
Eno2	1724,624	-0,973	3,52E-17
Eno3	1342,784	0,093	0,320762
Gapdh	55176,139	-0,651	2,00E-21
Gapdhs	26,701	-0,444	0,167964
Gpi1	43259,137	-0,737	9,41E-29
Pfkfb1	183,959	0,555	0,000402
Pfkfb2	201,167	-0,179	0,310899
Pfkfb3	4516,197	-0,879	3,72E-18
Pfkfb4	452,366	-0,206	0,081174
Pfkl	5780,410	0,013	0,918526
Pfkm	2590,051	-0,574	2,79E-12
Pfkp	27964,274	-0,396	5,54E-17
Pgam1	3991,382	-0,506	5,65E-15
Pgam2	0,217	-0,022	NA
Pgk1	26915,729	-0,573	3,63E-24
Pkm	77359,267	-0,470	1,01E-17
Ppp2ca	9023,452	0,097	0,172421
Ppp2cb	1889,221	0,197	0,006054
Ppp2r1a	8891,430	-0,034	0,647369
Ppp2r1b	2065,960	0,381	1,42E-05
Ppp2r5d	4135,747	0,010	0,91745
Tpi1	31117,420	-0,469	4,61E-20
Hk1	9339,402	-0,357	1,44E-10
Hk2	4793,555	-0,326	9,97E-08
Pdk1	7305,854	-0,635	8,82E-26
Pdk2	236,596	-0,626	5,56E-06
Pdk3	2582,943	-0,172	0,013768
Pdk4	4,221	0,112	0,761934
Ldha	65638,633	-0,184	0,001483
Ldhb	533,809	-0,098	0,423079

Fatty Acid Oxidation			
Gene	**baseMean**	**Log2(FC)**	**padj**
Eci1	1038,825	0,03	0,823425
Decr1	881,707	0,10	0,367756
Echs1	1859,201	-0,01	0,927409
Hadha	4933,294	-0,09	0,175124
Hadhb	1491,794	-0,30	0,000204
Hadh	2742,933	-0,31	8,17E-06
Acadl	5342,563	-0,07	0,327975
Acadm	1491,178	-0,31	1,93E-05
Acads	2123,329	-0,05	0,547946
Acavl	3572,967	-0,31	1,82E-06
Mut	872,377	0,29	0,003252
Pcca	1006,590	0,33	3,17E-05
Pccb	349,317	0,28	0,024875
Mcee	345,735	-0,02	0,912942
Acaa2	1534,607	-0,11	0,161566
Eci2	2353,759	-0,36	9,79E-07
Cpt1c	137,377	-0,27	0,17963
Cpt1a	1935,454	-0,11	0,15346
Cpt1b	16,273	0,23	0,558289
Cpt2	687,784	0,36	0,01039
Ehhadh	294,505	0,11	0,478236
Acaa1	1838,818	-0,16	0,058221
Acadsb	733,305	-0,32	0,003768
Acox1	1511,252	-0,39	3,66E-08
Acox3	1737,994	-0,19	0,015823

TCA cycle			
Gene	**baseMean**	**Log2(FC)**	**padj**
Cs	16189,47	0,078	0,178434
Dlat	2280,944	0,507	7,12E-13
Dld	3744,499	0,202	0,005728
Dlst	4465,023	0,355	1,36E-08
Fh1	2897,334	0,365	5,79E-08
Idh1	532,039	0,125	0,362948
Idh2	2445,576	0,136	0,049929
Idh3a	2767,437	0,749	5,71E-22
Idh3b	6058,123	-0,219	0,000505
Idh3g	4954,778	-0,157	0,013538
Mdh1	9533,532	0,061	0,331515
Mdh2	10750,29	0,303	1,81E-08
Acly	11399,52	0,380	4,47E-07
Aco1	1547,981	0,159	0,034605
Ogdh	6946,745	0,426	4,88E-11
Aco2	11011,63	0,384	1,47E-09
Pcx	1024,123	-0,194	0,082504
Pck1	0,388	-0,065	NA
Pck2	4993,493	-0,015	0,867056
Pdha1	7799,495	0,057	0,44297
Pdha2	0,695	0,059	NA
Pdhb	2699,068	0,122	0,133871
Ogdhl	11,469	0,240	0,5383
Sdha	8450,051	0,090	0,180022
Sdhb	4991,005	0,298	2,65E-06
Sdhc	3263,892	0,210	0,001346
Sdhd	5005,418	-0,047	0,5762
Suclg2	3304,283	0,151	0,017431
Suclg1	1372,262	0,456	1,61E-08
Sucla2	2068,636	0,232	0,00235

Pentose Phosphate Pathway			
Gene	**baseMean**	**Log2(FC)**	**padj**
Fbp1	0,326	0,035	NA
Aldoa	103491,4	-0,723	8,29E-26
Aldob	0,475379	0,027	NA
Rpia	1738,706	0,504	7,94E-11
Aldoc	5183,226	-0,942	8,75E-45
G6pdx	1905,487	0,478	1,04E-10
Pgls	1983,66	0,068	0,452368
Gpi	43259,14	-0,737	9,41E-29
Dera	1311,308	0,162	0,069359
Pfkl	5780,41	0,013	0,918526
Pfkm	2590,051	-0,574	2,79E-12
Pfkp	27964,27	-0,396	5,54E-17
Pgd	2973,471	0,299	6,40E-06
Pgm1	1309,232	0,087	0,342272
Pgm2	5487,737	-0,776	5,83E-47
Prps1	3075,289	0,613	2,77E-17
Rpe	2126,647	0,052	0,674531
Rbks	81,88351	0,268	0,25233
Taldo1	4123,064	0,371	2,64E-09
Tkt	20112,71	0,144	0,008331
Tktl1	0,314299	0,043	NA
H6pd	928,0053	0,179	0,132816

Fatty Acid Synthesis			
Gene	**baseMean**	**Log2(FC)**	**padj**
Acsl1	402,804	0,524	8,30E-06
Acsl3	1585,043	-0,335	0,000155
Acsl4	6238,057	0,073	0,352829
Fasn	10487,04	0,575	1,62E-09

Acsl6	259,068	0,382	0,004425
Acaca	1929,027	0,530	2,43E-09
Acly	11399,52	0,380	4,47E-07
Acsl5	8223,055	0,320	1,80E-05
Elovl2	0,217275	-0,022	NA
Elovl5	5620,83	-0,223	0,00049
Elovl1	2254,533	0,206	0,004595
Slc25a1	3386,888	0,066	0,449895
Elovl4	46,28493	0,268	0,364521
Elovl6	2086,301	0,098	0,294691
Elovl7	175,5459	-0,184	0,298221
Elovl3	0,217275	-0,022	NA
Tecr	5379,159	-0,008	0,926046

OXPHOS			
Gene	**baseMean**	**Log2(FC)**	**padj**
Cox17	1964,352	-0,068	0,505579
Tcirg1	3345,265	-0,315	0,000363
Atp5h	4378,264	-0,046	0,618091
Atp5l	25,313	-0,317	0,349105
Uqcr11	1028,659	0,432	8,48E-08
Cox6b2	4434,789	0,052	0,576087
Cox6b1	1005,278	-0,042	0,708435
Ndufa11	1169,968	0,125	0,180214
Atp6v1g3	1,503	0,093	NA
Cox4i1	8452,615	-0,007	0,932118
Cox5b	2335,219	0,277	7,96E-05
Cox6a1	4974,910	0,098	0,221445
Cox6a2	66,277	-0,546	0,017437
Cox6c	3523,931	0,067	0,350515
Cox7a1	58,916	-0,591	0,012521
Cox7a2	3897,642	0,021	0,821056
Cox7b	4188,318	0,143	0,038435
Cox7c	2373,819	-0,111	0,142367
Cox8a	6971,659	0,144	0,094239
Cox10	954,024	0,455	1,06E-06
Cox11	341,977	0,060	0,716475
Cox15	1979,146	0,366	5,18E-06
Cyc1	4224,080	0,395	3,39E-10
Atp6v0e2	8,647	0,023	0,96075
Atp6v0d2	47,649	-0,627	0,017431
Atp6v0c	407,467	0,049	0,744093
Atp6v0a2	2736,286	-0,034	0,681515
Ppa2	1075,047	0,484	6,73E-09
Uqcrq	3098,858	0,363	2,69E-08
Uqcr10	2889,556	0,229	0,001124
Ndufs7	1940,704	0,240	0,000967
Atp5g1	1377,818	0,340	0,000201
Uqcrh	5986,371	-0,413	2,07E-10
Atp6ap1	2559,384	-0,203	0,002009
Atp6ap2	1723,958	0,074	0,486746
Atp8a1	963,584	0,015	0,905345
Atp8a2	4,578	-0,075	0,852361
Atp8b1	3,840	0,339	0,269039
Atp8b2	4088,716	-0,073	0,352986
Atp8b3	4,099	0,251	0,454583
Atp8b4	2570,883	0,504	1,60E-09
Atp8b5	1,370	0,287	NA
mt-Cytb	22221,01	0,823	1,32E-18
mt-Nd1	33925,56	0,681	2,16E-14
mt-Nd2	17186,5	0,831	5,51E-26
mt-Nd3	0,312617	-0,007	NA
mt-Nd4	12136,11	1,019	1,97E-34
mt-Nd5	32034,17	0,505	3,19E-13
mt-Nd6	478,9847	-0,118	0,518287
Ndufa1	1230,159	0,078	0,431752
Ndufa2	1872,867	0,024	0,827937
Ndufa3	1843,684	-0,064	0,519346
Ndufa4	2960,172	0,430	3,64E-09
Ndufa5	685,976	0,510	5,59E-06
Ndufa6	3225,860	-0,476	9,77E-11
Ndufa7	2388,900	0,086	0,335355
Ndufa8	1896,458	0,180	0,031362
Ndufa9	3370,989	0,142	0,033198
Ndufa10	3844,788	0,167	0,013211
Ndufab1	1324,281	0,165	0,065138
Ndufb2	446,510	0,090	0,524516
Ndufb3	1496,502	0,159	0,087788
Ndufb4	174,510	-0,017	0,940166
Ndufb5	3144,335	-0,053	0,562127
Ndufb6	1768,196	0,282	7,65E-05
Ndufb7	2296,584	0,201	0,017199
Ndufb8	1972,416	0,284	7,12E-05
Ndufb9	2163,668	0,145	0,077446
Ndufb10	2013,452	0,005	0,963281
Ndufc1	813,532	0,220	0,014329
Ndufc2	2077,259	0,196	0,005062
Ndufs1	3301,934	0,254	5,53E-05
Ndufs2	5345,807	-0,067	0,365521
Ndufs3	1842,350	-0,231	0,010045
Ndufv1	3085,312	0,300	1,13E-05
Ndufs4	1832,786	-0,107	0,169394
Ndufs5	364,942	0,378	0,00283
Ndufs6	1536,132	0,274	0,003365
Ndufs8	2133,126	0,152	0,070945
Ndufv2	3461,655	0,000	0,998692
Ndufv3	4133,567	-0,719	1,46E-15
Atp12a	0,444	0,081	NA
Atp4a	31,033	-0,297	0,356811
Atp5a1	28843,98	0,274	3,95E-07
Atp5b	44431,05	0,296	3,87E-08
Atp6v0a4	0,161	-0,022	NA
Atp5c1	11085,92	-0,095	0,118576
Atp5d	8878,947	-0,123	0,089551
Atp6v1d	1990,617	-0,325	0,000127
Atp5e	3896,595	-0,086	0,306654
Atp5f1	8265,778	0,142	0,033687
Atp6v1h	1735,166	-0,048	0,637174
Atp5g2	1213,286	-0,062	0,567009
Atp5g3	6633,098	0,384	6,30E-11
Atp5j	3731,915	0,464	6,86E-12
Atp6v1a	4688,973	0,009	0,929678
Atp6v1b1	0,957	-0,091	NA
Atp6v1b2	2826,001	-0,080	0,300557
Atp6v1c1	1403,512	0,228	0,004893
Atp6v1e1	1761,911	0,028	0,775319
Atp6v0b	1814,302	-0,330	0,000318
Atp6v1g2	238,867	-0,210	0,158356
Atp6v0a1	836,167	-0,052	0,650468
Atp5o	4406,529	0,065	0,365542
Ppa1	2741,897	0,852	1,91E-22
Ndufa4l2	1,698	-0,039	NA
Sdha	8450,051	0,090	0,180022
Sdhb	4991,005	0,298	2,65E-06
Sdhc	3263,892	0,210	0,001346
Sdhd	5005,418	-0,047	0,5762
Lhpp	201,855	0,338	0,035831
Uqcrb	1843,160	0,177	0,038531
Uqcrc1	6231,243	0,381	7,19E-11
Uqcrc2	9614,012	0,075	0,240748
Uqcrfs1	3973,641	0,147	0,028167
Cox4i2	33,026	-1,445	8,48E-08
Atp6v0e	2408,840	-0,361	6,14E-06
Atp6v0d1	1908,879	-0,256	0,000316
Cox7a2l	4357,751	-0,474	4,64E-10
Atp6v1f	1932,605	-0,049	0,618655
Cox5a	5347,093	0,266	1,71E-05

Atp6v1g1	1220,312	-0,160	0,072462
Atp5j2	3705,844	-0,008	0,936343

	cMyc-dependent metabolic genes			
Gene	**pathway**	**BaseMean**	**Log2(FC)**	**padj**
Slc38a1	Glutaminolysis	7157,442	0,169	0,02914
GOT1	Glutaminolysis	4559,558	0,118	0,06312
GOT2	Glutaminolysis	4487,491	0,232	0,00020
PPAT	Glutaminolysis	2841,507	0,467	9,13E-09
GPT	Glutaminolysis	210,335	-0,040	0,84721
Gls2	Glutaminolysis	825,873	-0,754	2,92E-11
Gls	Glutaminolysis	6436,671	-0,103	0,31407
Slc1a5	Glutaminolysis	9791,542	0,400	6,79E-06
ME2	Glutaminolysis	4147,997	-0,238	0,00096
slc3a2	Glutaminolysis	10778,388	-0,020	0,82153
slc7a5	Glutaminolysis	12075,357	0,389	2,05E-07
Slc16a1	Glycolysis	3898,558	0,299	4,00E-05
Slc2a3	Glycolysis	24963,571	-1,186	1,88E-73
Glud1	Glycolysis	9749,808	-0,065	0,32978
LDhb	Glycolysis	533,809	-0,098	0,42307
Eno1	Glycolysis	38419,091	-0,313	9,75E-07
Slc16a3	Glycolysis	6134,605	-0,573	9,17E-19
PGK1	Glycolysis	26915,729	-0,573	3,63E-24
GPI	Glycolysis	43259,137	-0,737	9,41E-29
Pgam1	Glycolysis	3991,382	-0,506	5,65E-15
Slc2a1	Glycolysis	5610,559	-0,858	1,04E-22
Gpd1l	Glycolysis	1237,190	0,517	1,70E-10
Pfkl	Glycolysis	5780,410	0,013	0,91852
HK2	Glycolysis	4793,555	-0,326	9,97E-08
LDHa	Glycolysis	65638,633	-0,184	0,00148
Aldoa	Glycolysis	103491,44	-0,723	8,29E-26
Tpi	Glycolysis	31117,420	-0,469	4,61E-20
Pfkfb3	Glycolysis	4516,197	-0,879	3,72E-18
Pkm	Glycolysis	77359,267	-0,470	1,01E-17
Aldh18A1	Polyamine	7555,299	0,276	3,62E-06
Sms	Polyamine	1863,269	0,217	0,004338
Odc1	Polyamine	9807,048	0,369	1,41E-10
Prodh	Polyamine	102,935	0,990	2,16E-07
GFPT1	Polyamine	5190,251	-0,181	0,004291
OAT	Polyamine	3385,538	0,121	0,09745
Srm	Polyamine	3159,278	0,911	1,96E-25
TKT	PPP	20112,705	0,144	0,008331
G6PDx	PPP	1905,487	0,478	1,04E-10
IDH3a	TCA	2767,437	0,749	5,71E-22
IDH3b	TCA	6058,123	-0,219	0,000505
IDH3g	TCA	4954,778	-0,157	0,013538
SDHc	TCA	3263,892	0,210	0,001346
SDHd	TCA	5005,418	-0,047	0,5762
PDHx	TCA	551,803	0,447	3,69E-06
Dlat	TCA	2280,944	0,507	7,12E-13
MDH2	TCA	10750,290	0,303	1,81E-08
Arg1	Ureacycle	2,149	-0,012	NA
Arg2	Ureacycle	3,000	-0,050	NA
Nos1	Ureacycle	6,412	0,464	0,156246
Nos2	Ureacycle	340,431	-1,392	3,32E-22

Table S1. Raw data from RNAseq analysis of control and Drp1 KO T cells. Related to Figure 3 and Supplemental Figure 3.

Raw data from RNAseq analysis of the genes reported in Fig. 3F-G and S3E. For each gene the following data are reported: mean count value between KO and control (3 samples each) (Base Mean); logarithmic value of the Fold Change between the mean value of KO and controls (Log2FoldChange); adjusted p-value (padj).